

Sodium ion and cobalt charge ordering in Na_xCoO_2 ($x \sim \frac{5}{6}$)

P. Foury-Leylekian,¹ V. V. Poltavets,² N. Jaouen,³ J.-P. Rueff,^{3,4} J. E. Lorenzo,⁵ P. Auban-Senzier,¹ C. R. Pasquier,¹ C. Mazzoli,⁶ and M. Greenblatt²

¹Laboratoire de Physique des Solides (CNRS-UMR 8502), Université Paris-Sud, Bâtiment 510, 91405 Orsay Cedex, France

²Department of Chemistry and Chemical Biology, Rutgers, The State University of New Jersey, Piscataway, New Jersey 08854, USA

³Synchrotron SOLEIL, L'Orme des Merisiers, Saint-Aubin-BP 48, 91192 Gif-sur-Yvette Cedex, France

⁴CNRS, UMR 7614, Laboratoire de Chimie Physique-Matière et Rayonnement, F-75005 Paris, France

⁵Institut Néel, CNRS, BP 166, 38042 Grenoble, France

⁶European Synchrotron Radiation Facility, 38043 Grenoble, France

(Received 21 October 2008; revised manuscript received 26 January 2009; published 3 March 2009)

We present a direct study of the Co charge order and Na ordering in three Co-layers Na_xCoO_2 ($x \sim \frac{5}{6}$) single crystals. From diffuse scattering measurements, we propose a model of Na supercell which rules out the ones previously suggested in parent cobaltates with double Co layers. Via a direct measurement of the Co charge state using anomalous x-ray scattering, we also evidence a Co charge order which evolves between 200 and 290 K.

DOI: 10.1103/PhysRevB.79.115101

PACS number(s): 71.30.+h, 61.05.C-, 71.45.Lr

I. INTRODUCTION

Sodium cobaltates Na_xCoO_2 have been intensively studied since the 1980s for their potential application as ionic conductors in batteries¹ and more recently for their exceptionally large thermoelectric power.^{2,3} The discovery of a superconducting ground state in the hydrated $\text{Na}_{0.35}\text{CoO}_2 \cdot 1.4\text{H}_2\text{O}$ (Ref. 4) has renewed interest in this family of materials, bringing new focus to their unusual structural and electronic properties, in many aspects similar to the extensively studied cuprates. The structure of Na_xCoO_2 consists of edge sharing cobalt-oxygen octahedra that form a triangular net of Co ions intercalated with sodium layers. The CoO_2 planes are the key components of the sodium cobaltates, embodying both low dimensional electronic properties and strong correlations (due to high electron doping via the Na layers). In the highly doped region ($x \geq 0.5$), the phase diagram is characterized by the coexistence of itinerant and localized electrons as well as the presence of magnetic orders at low temperature. Albeit the origin of such a complexity is not fully understood, it is thought to be a manifestation of the interplay between spin, charge, and orbital degrees of freedom. The charge degree of freedom that takes place at the Co sites originates from the Na^+ ions, while the orbital degrees of freedom are due to the crystal-field splitting of the Co $3d$ levels into e_g and t_{2g} states.^{5,6} The strength of the crystal field also forces the two Co ions [nominally $\text{Co}^{3+}(t_{2g}^6 e_g^0)$ and $\text{Co}^{4+}(t_{2g}^5 e_g^1)$] to adopt low-spin electronic configurations, respectively, $S=0$ and $S=1/2$. The associated spin entropy supposedly leads to the enhanced thermoelectric power reported in this material.⁷

Complexity is further introduced by the presence of disorder-order transitions in the alkali layers,⁸⁻¹¹ (also observed in other parent cobaltates¹²). Na was reported to form a long-range superstructure whose pattern is well accounted for by electrostatic interactions and the amount of Na vacancies in the lattice. This finding has, in turn, triggered intense interest in searching for a charge ordering of the Co layers for its far-fetched implications on the electronic properties.

Co charge ordering has been theoretically predicted,^{6,13} but lacks experimental evidence, although NMR has provided a hint of charge disproportionation between Co^{3+} and $\text{Co}^{3+\delta}$ states in compounds $x > 0.65$.¹⁴⁻¹⁷ The Co charge-ordered state also brings up new questions that call for clarification: what is its origin and exact nature; is it an intrinsic instability or a consequence of the Na order?

A good starting point to understand the interplay between the cobalt and sodium layers is to have a reliable description of the sodium ordering. However, the proper characterization of the Na ordering pattern faces several difficulties, especially in the highly doped region ($x \geq 0.8$). First, the Na ordering depends on the exact Na content, a quantity difficult to control due to Na diffusion and aggregation. Second, the Na order is very sensitive to the morphology of the compound.¹⁸ In polycrystalline samples, the Na superstructures form an orthorhombic supercell^{19,20} while in single crystals, quasihexagonal supercells (m^*m) (Refs. 11, 21, and 22) or more complex superlattice²² have been proposed. Finally, the Na ordering also depends on the average structure of the cobaltate which can be either a quasirhombohedral three Co-layers structure^{20,23,24} or a hexagonal double Co-layers structure.

In this paper, we address the questions of both Na and Co charge ordering in Na_xCoO_2 ($x \sim \frac{5}{6}$) a model three Co-layers compound. Na ordering was investigated by x-ray diffuse scattering whereas Co charge order was studied by anomalous scattering at the Co K edge. The measurements have been carried out on single crystals. These are essential to extract information from anomalous scattering, and also minimize the effects of moisture sensitivity.

II. EXPERIMENTAL DETAILS

A. Synthesis

Single crystals of $\text{Na}_{0.83}\text{CoO}_2$ were prepared by a flux method. Co_3O_4 (Sigma-Aldrich, 99.8%), Na_2CO_3 (Sigma-Aldrich, 99.5%), and NaCl (Fluka, 99.5%) powders were

mixed in the nominal weight ratio of $\text{Co}_3\text{O}_4:\text{Na}_2\text{CO}_3:\text{NaCl}=1:2:5$. The mixture was heated to 1050°C in an alumina crucible in air and slowly cooled to 800°C at a rate of 3°C/h . The obtained hard lump was washed with anhydrous methanol until it broke into powder due to NaCl grain boundaries dissolving. Black platelike crystals of Na_xCoO_2 of sizes up to $5\times 5\times 0.5\text{ mm}^3$ were isolated under the optical microscope.

B. Characterization

Na_xCoO_2 ($x\sim\frac{5}{6}$) is hygroscopic, and the Na content is difficult to control, thus an accurate chemical characterization of the samples is essential.

Concerning the purity of the crystals, Na_xCoO_2 single crystals grown from $\text{Co}_3\text{O}_4:\text{Na}_2\text{CO}_3:\text{NaCl}=1:2:5$ mixtures were reported to have good quality. In particular, no aluminum impurity from the alumina crucible as determined by scanning electron microscopy-energy dispersive x-ray.²⁵

The average structure of several single crystals was determined with x-ray diffraction. For all the crystals, the space group has been determined to be $C2/m$ with unit-cell parameters $a_M=0.490\text{ nm}$, $b_M=0.287\text{ nm}$, $c_M=0.576\text{ nm}$, and $\beta_M=111.9^\circ$ (the index gives the type of system—here monoclinic). This result is in good agreement with previously published results for three-Co-layers cobaltates.^{8,20,23} The value of c_H [deduced from the measurement by the formula $c_H=2^*c_M^*\sin(\beta)$] is slightly smaller than the one reported for $\text{Na}_{0.75}\text{CoO}_2$, which indicates a Na content slightly above $x=0.75$. In these highly Na doped three-Co-layers compounds, the ideal rhombohedral structure is weakly distorted into a monoclinic one. However, the distortion is very small, so the primitive unit cell of the C -centered monoclinic structure is very similar to that of the rhombohedral structure. In the following, we will only use the primitive unit cells. The primitive cell of the crystals measured is of triclinic symmetry $P\bar{1}$ with unit-cell parameters $a_t=0.284\text{ nm}$, $b_t=0.287\text{ nm}$, $c_t=0.576\text{ nm}$, $\alpha_t=90^\circ$, $\beta_t=108.6^\circ$, and $\gamma_t\approx 120^\circ$.

Superconducting quantum interference device (SQUID) measurements at 1.5 T have been performed on several single crystals of the same batch. The Na content can also be inferred from the measurement of sodium-sensitive parameters such as the Curie-Weiss constant and the critical temperature of the low-temperature magnetic transition. For all the samples measured, the results were similar indicating the sodium homogeneity of the batch and of the crystals. The Curie constant has been determined to be around $6.10^{-2}\text{ emu/mol K}$ and the critical temperature of the magnetic transition $T_c=25\text{ K}$. This result is in agreement with those obtained on three-Co-layers compounds with a range of Na composition 0.75 (Ref. 23)–0.85 (Ref. 26). It is also in good agreement with the results obtained on double-Co-layers of $x\sim 0.85$.²⁷

From the previous characterizations, we have thus estimated the Na content of the crystals studied in this work, to be around 0.8 ± 0.05 a value very close to the ideal commensurate $x\sim\frac{5}{6}$ value.

Resistivity measurements in the (a,b) plane have also been performed using a standard four points low-frequency

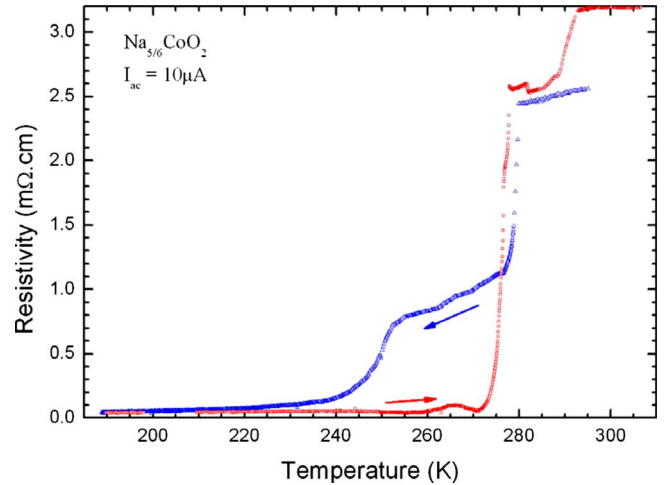


FIG. 1. (Color online) Temperature dependence of the resistivity measured in the (a,b) plane upon cooling (blue curve) and upon heating (red curve).

lock-in technique with an applied current of $10\ \mu\text{A}$. Two samples of the same chemical batch have been measured. The results slightly differ upon the sample. In addition, the reactivity to air of the crystal surface prevents complete reproducibility of the resistivity measurement on the same sample after one temperature cycle. In both samples the $\rho(T)$ curve shows metallic behavior with several steps in the temperature range between 250–300 K (see Fig. 1). Upon cooling two main steps are observed at $250\pm 2\text{ K}$ and $280\pm 2\text{ K}$; while upon heating three steps are observed at $265\pm 2\text{ K}$, $275\pm 2\text{ K}$, and $290\pm 2\text{ K}$. This steplike behavior recalls a first-order phase transition with an hysteresis in a temperature range including the room temperature. It is important to notice that these anomalies are similar to the ones reported in transport and NMR studies performed on double Co-layers compounds^{9,11,15,18} and attributed to Na rearrangements.

C. High resolution electron microscopy

High resolution electron microscopy images and diffraction patterns were acquired with a TOPCON 002B TEM fitted with UHR pole pieces on a home-made charge-coupled device (CCD) camera. Diffraction patterns were obtained in the select area mode that allows the isolation of a circular area ca 300 nm in diameter. For both images and diffraction patterns the electron gun was operated at 100 kV. The samples studied by electron microscopy were single crystals gently ground under hexane.

D. Diffuse scattering experiment

The study of the Na superstructure has been performed with the so-called fixed-film fixed-crystal x-ray diffuse scattering technique. The molybdenum wavelength ($\lambda=0.0709\text{ nm}$) has been used. At this energy, the penetration length in the Na_xCoO_2 compounds is about $\sim 100\ \mu\text{m}$, which corresponds to the crystal thickness. The structural investigation has been carried out in the temperature range

20–335 K with a cryocooler. Several samples (about 10) of the same composition batch have been studied to check the reproducibility.

E. Anomalous scattering experiment

In contrast to Na ordering, the atomic displacements associated with the Co charge ordering are too weak to be observed using diffuse scattering. The occurrence of a charge order among the Co cations was studied by anomalous x-ray scattering at the Co *K* edge. In anomalous x-ray scattering the energy dependence of the scattered intensity of selected reflections is measured around the absorption edge of one of the chemical species in the compound. The anomalous signal comes from absorption/emission coherent processes associated with electronic transitions between core atomic levels and unoccupied electronic states near the Fermi level. In the present case at the Co *K* edge, the electronic transitions involve both dipolar-dipolar ($1s \rightarrow 4p \rightarrow 1s$) and quadrupolar-quadrupolar ($1s \rightarrow 3d \rightarrow 1s$) channels. Both transitions are sensitive to the charge order on the Co site although quite often the latter ones are weaker than the former ones. In our Na_xCoO_2 system, three scenarios can be expected: either a homogeneous valence state Co^{4-x} for all the Co ions, or a disordered array of two Co charge states, or finally a Co charge order with different species such as Co^{3+} and $\text{Co}^{3+\delta}$. Whereas the two first scenarios will not give a significant enhancement of the scattering at the resonance, the charge order will give rise to specific features in the energy dependence of the scattering. In this case, the anomalous scattering factors f of the different species will be globally shifted in energy between each other in such a way that: $f^{3+\delta}(E + \delta E) = f^3(E)$. Thus, the Bragg reflections formed from the subtraction of the anomalous scattering factors of the two charged species will have a “derivative aspect” with two lobes of opposite sign while showing a high sensitivity to the charge differences between the same chemical species. We will refer to this difference as charge disproportionation.^{28,29} Notice that if the charge disproportionation is strong and the phase factors of both charge states are globally of the same sign for a given Q position, the scattering factors of both species may add up instead, yielding energy spectra with two peaks, one for each particular charge state. Clearly, the latter scenario better matches the experimental spectra as discussed in Sec. III B.

Experiments were performed at the ID20 beamline at the European Synchrotron Radiation Facility (Grenoble, France).³⁰ A crystal of about $0.1 \times 0.2 \times 2 \text{ mm}^3$ was mounted on a five-circle diffractometer in a closed-cycle refrigerator (Displex) operating from 310 to 16 K. The x-ray beam wavelength was set by a Si(111) double crystal monochromator with an energy resolution of 1 eV. No polarization detection was performed, but a (002) pyrolytic graphite analyzer was used to reduce fluorescence background. Data were collected near the Cobalt *K* edge (7720 eV) typically between 7650 and 7800 eV with steps of 0.5 eV. The fluorescence spectrum has been systematically recorded for absorption corrections. In addition, the energy spectrum of the (003) and (004) Bragg reflections near the studied satellite

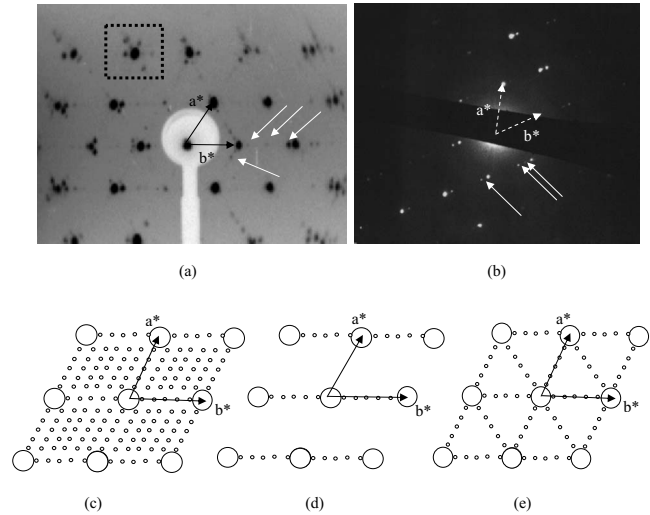


FIG. 2. (a) X-ray pattern of a single crystal from the composition $\text{Na}_{0.83}\text{CoO}_2$. The reciprocal unit cell is indicated by black arrows. The satellite reflections related to the Na ordering are indicated by white arrows. The satellite reflections form hexagon around the Bragg reflections as shown inside the dotted square. (b) TEM diffraction pattern from a ground crystal of the same composition. The satellite reflections are indicated by white arrows. The satellite reflections are only located along the b^* direction. (c) Reciprocal lattice of a 6^*6^*1 superstructure. (d) Reciprocal lattice of a 1^*6^*1 superstructure in the case of a single crystal. (e) Same as (d) but is the case of a twinned crystal. The pattern is the superposition of three reciprocal lattices (d) rotated by 120° .

reflections have also been recorded to improve the absorption corrections.

III. DESCRIPTION AND ANALYSIS OF THE RESULTS

A. Study of the sodium ordering

At 290 K, the x-ray patterns of almost all the crystals studied by diffuse scattering were similar. Figure 2(a) shows a typical x-ray pattern. The main Bragg reflections form the expected two-dimensional (2D) quasi-hexagonal lattice. Weak additional reflections are also observed. Their intensity is about 5×10^{-2} that of the main Bragg reflections. The satellite reflections seem to be associated with the Na ordering, which is expected to settle between 250 and 400 K.^{9–11} The width of the satellite reflections corresponds to the experimental resolution (0.2 \AA^{-1}). No diffuse scattering related to any kind of disorder has been detected. This indicates long-range order of the Na ions and furthermore it proves the homogeneity of the Na distribution in our samples.

The satellite reflections are essentially located along the three quasidequivalent $\langle 100 \rangle$ directions of the quasihombohedral lattice at commensurate positions $q = n/6 \langle 100 \rangle$ ($n = 1$ to 5). Thus, the satellite reflections form hexagons around the Bragg reflections [see dashed square in Fig. 2(a)]. In this system, the presence of twins is frequently observed.¹⁹ The twins are related by a rotation of 120° around the *c* axis. The x-ray pattern of a twinned crystal is then expected to be made up of the superposition of the patterns of the three

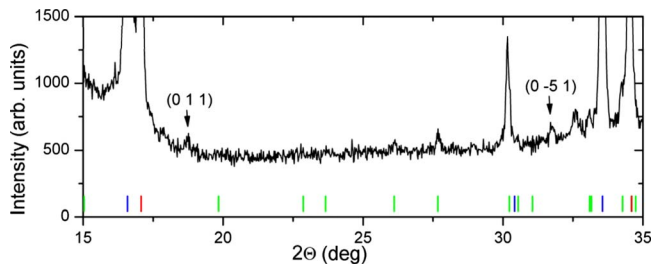


FIG. 3. (Color online) X-ray powder-diffraction pattern of ground single crystals of the composition $\text{Na}_{0.83}\text{CoO}_2$. The vertical blue ticks mark the positions of the Bragg reflection from the mean structure. The Bragg reflections of parasite phases NaCoO_2 (red ticks) and Na_2CoO_3 (green ticks) are also present in the pattern. The two superlattice reflections associated to the Na ordering in the $\text{Na}_{0.83}\text{CoO}_2$ phase are indicated by arrows.

twins. This difficulty prevents us from concluding between two possible superstructures built up from either 6^*6^*1 quasirhombohedral or 1^*6^*1 (or the nearly equivalent 6^*1^*1) supercells. The reciprocal pattern expected for a 6^*6^*1 superstructure is presented in Fig. 2(c). Notice that the reciprocal lattice of the single crystal is here identical to that of the twinned crystal. This differs from the 1^*6^*1 superstructure presented in Figs. 2(d) and 2(e) for a single crystal and a twinned crystal, respectively.

As inferred from Fig. 2(c), the reciprocal lattice of the 6^*6^*1 supercell is very dense, showing satellite reflections along and between the three $\langle 100 \rangle$ quasiequivalent directions. This pattern clearly contrasts with that observed experimentally [Fig. 2(a)], although one cannot rule out extinctions due to structure factor effects. On the other hand, the reciprocal lattice of the 1^*6^*1 superstructure obtained for a twinned crystal [Fig. 2(e)] clearly fits the experimental results. In order to definitively conclude between the two possible superstructures, we have performed a transmission electron microscopy study on ground single crystals. Among all the grains obtained from the grinding, some were still twinned. However, several grains had remained single crystals. The diffraction pattern of untwinned crystals is presented in Fig. 2(b). The satellite reflections are observed only along one of the three quasiequivalent $\langle 100 \rangle$ directions which undoubtedly exclude the possibility of a 6^*6^*1 superstructure.

It is important to notice that in this system, a 1^*6^*1 supercell is not strictly equivalent to a 6^*1^*1 one due to the monoclinic distortion of the ideal rhombohedral average structure. An accurate measurement is necessary to distinguish between these two possibilities. Because of the large mosaic spread of the single crystals, a powder x-ray measurement on ground single crystals was found to be the most suitable for this analysis. From the presence of at least two superstructure lines (see Fig. 3) we can unambiguously conclude that the superstructure is built from 1^*6^*1 supercells.

We can also compare our result with those previously published on similar systems $x \sim 0.8$.^{11,22} All the studies yield very similar results: the reciprocal patterns are all consistent with superstructure reflections forming hexagons around the Bragg reflections. However, our interpretation is substantially different than those proposed in the other papers. The

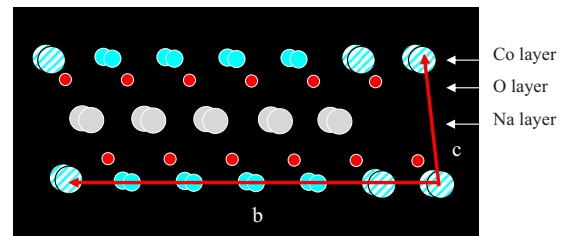


FIG. 4. (Color online) Schematic of the 1^*6^*1 supercell associated with the Na ordering already present at 300 K. The nature of the different atoms is indicated in the figure. The Na vacancy is located in the first subcell. The Co atoms represented by hatched circles are supposed to be in a $\text{Co}^{3.5}$ mixed state, the others are supposed to be in a Co^{3+} state.

discrepancy is essentially related to the fact that the twinning effect, required for the correct understanding of the experimental patterns, was neglected in all the previous studies. Thus, the 5^*5^*1 hexagonal-supercell proposed in Ref. 11 for $x \sim 0.75$ compounds can be described as a twinned 1^*5^*1 supercell, very close to the one evidenced in this work.

Based on these results, one can now build up a possible model for the Na superstructure. The 1^*6^*1 primitive supercell is of triclinic symmetry with unit-cell parameters $a_t = 0.284$ nm, $b_t = 1.722$ nm, $c_t = 0.5759$ nm, $\alpha_t = 90^\circ$, $\beta_t = 108.65^\circ$, and $\gamma_t \approx 120^\circ$. It contains six nonsymmetry equivalent Na sites and the same number of Co sites. In this picture, a Na concentration of $x = 0.80 \pm 0.05$ can be realized (within the error bars) from a $5/6$ commensurate concentration. In this case, one Na vacancy has to be inserted every six atoms and the Na ordering corresponds to the ordering of these Na vacancies. Because the 1^*6^*1 supercell preserves the a and c periodicities, only one model is possible. It is schematized in Fig. 4. The superstructure is composed of (a, c) planes of Na vacancies, forming stripes similar to those seen in polycrystalline samples.^{20,23} In addition to the order-disorder transition, a displacement of the atoms surrounding the Na vacancies can also be expected. This additional structural effect could explain the satellite reflections that have been observed even at high diffraction angle, which is unexpected for standard order-disorder transitions.

From the superstructure model proposed here, one can expect a higher charge for the Co occupying the two different Co sites surrounding the Na vacancy (indicated by hatched circles in Fig. 4). Furthermore, according to NMR measurements,^{16,17} there are Co^{3+} states in the system. A simple model of charge order can thus be assumed with Co atoms occupying the four Co sites far from the Na vacancies in a Co^{3+} valence state and Co atoms occupying the two Co sites near the Na vacancies in a $\text{Co}^{3.5+}$ mixed-valence state (see Fig. 4).

Upon cooling down to 25 K, the x-ray pattern remains nearly unchanged. No additional structural transition is detected. However, this observation does not exclude neither a Co charge rearrangement, which is very difficult to detect by diffuse scattering, nor the appearance of a Na rearrangement. In order to investigate the possible occurrence of Co charge order, an anomalous scattering experiment has been performed.

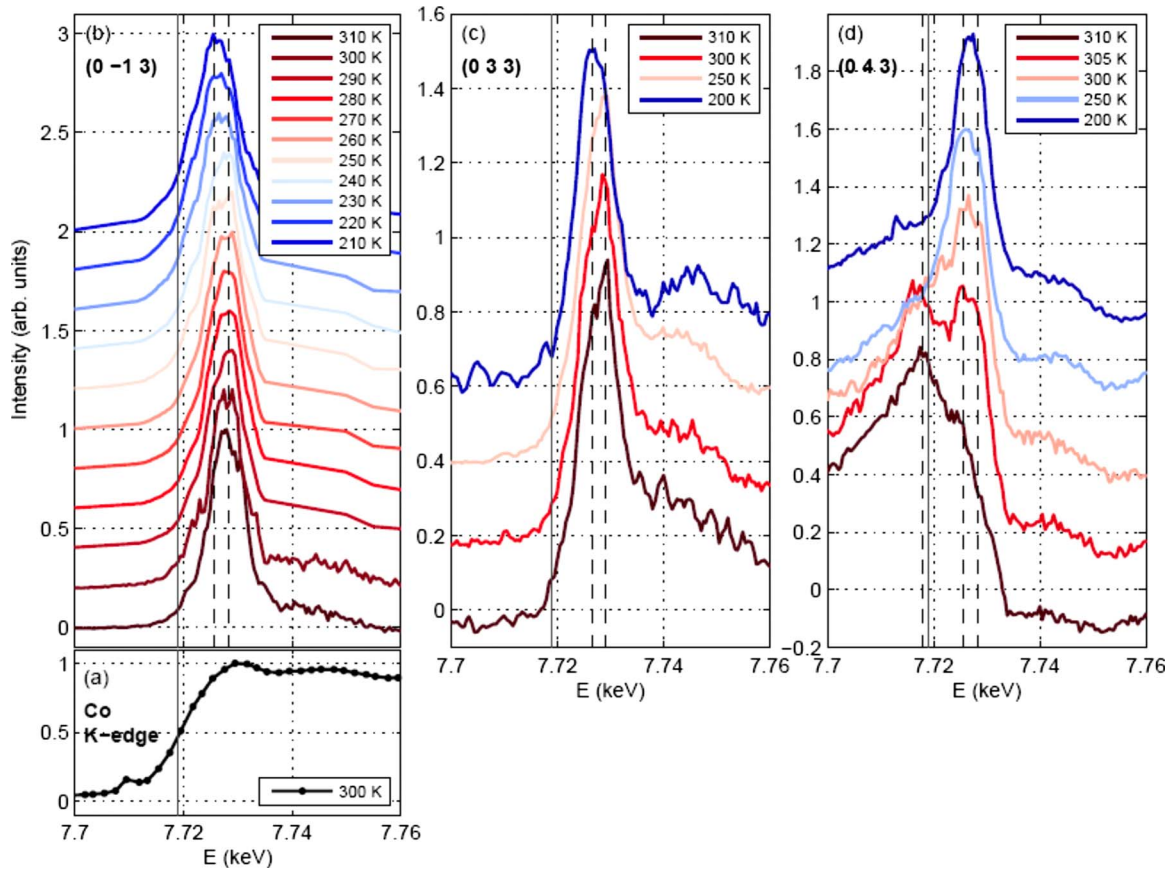


FIG. 5. (Color online) X-ray absorption near-edge structure (XANES) spectrum of $\text{Na}_{0.8}\text{CoO}_2$ at the Co K edge (a), energy spectra (solid line) of the $(0\bar{1}3)$ (b), $(0\bar{3}3)$ (c), and $(0\bar{4}3)$ (d) as a function of the incident energy. The different colors in Figs. 5(b)–5(d) correspond to different temperatures. The diffraction intensity is divided by the intensity of the (004) Bragg reflection for absorption correction. The diffraction spectra are further normalized to their maximum and translated vertically for clarity. The dashed lines indicate the position of the structures composing the resonant peak, and the solid line the position of the absorption edge.

B. Study of the cobalt charge order

Figure 5 summarizes the anomalous scattering experiment. The intensity of the $(0\bar{1}3)$, $(0\bar{3}3)$ and $(0\bar{4}3)$ (the indices are given in the supercell setting) satellite reflections have been recorded as a function of the incident photon energy around the Co K edge. The measurement has been performed in the temperature range 200–310 K where the Co charge order and the Na rearrangement are expected.^{9–11} The absorption spectrum is shown in Fig. 5(a) as a reference for the energy scale. The Co edge is defined by the inflection point of the absorption spectrum and is located at 7719.5 ± 0.5 eV. A prepeak is also visible at 7707.5 ± 0.5 eV, in agreement with our previous results in the Na_xCoO_2 series.³¹ Note that at the Co K edge, the penetration length is about $30 \mu\text{m}$. For this reason, Na superstructure reflections investigation has been repeated in resonant condition and found in perfect agreement with the results deduced from bulk diffuse scattering analysis.

The resonant scattering spectra for the different temperatures are presented in Figs. 5(b)–5(d). The raw data have been divided by the intensity of the (004) Bragg reflection to correct for the absorption.²⁹ We observe a strong anomalous effect for all the measured satellite reflections. As previously

explained, the anomalous effect in itself provides clear evidence of a Co charge order. For the $(0\bar{1}3)$ and the $(0\bar{3}3)$ reflections, the spectra are characterized by a double-peak structure peaking at $E_L=7725.5$ eV and $E_H=7728.5$ eV. The position of these two features above the Co K edge ($E=7719.5$) shows that the reflections measured are not sensitive to the charge difference—otherwise a peak centered exactly at the resonance energy would be observed—but to each Co charge states of the system as expected in the case of a strong charge disproportionation. Thus, the double-peak feature observed at the $(0\bar{1}3)$ and the $(0\bar{3}3)$ reflections could be assigned to a charge order of two different Co valences, already present at 290 K. It is interesting to notice that in the case of the $(0\bar{4}3)$ reflection, in addition to the double peak above the Co K edge, a broad structure is observed exactly at the Co edge. This reflection can be sensitive to both the charge disproportionation and the two different Co charge states.

In addition, a strong thermal dependence of the anomalous effect is observed for all the measured reflections. We focus more particularly on the $(0\bar{1}3)$ satellite reflection, which shows the largest sensitivity to temperature change (Fig. 6). The two structures of the anomalous peak are labeled peak L and peak H in Fig. 6(a). Upon heating from 200

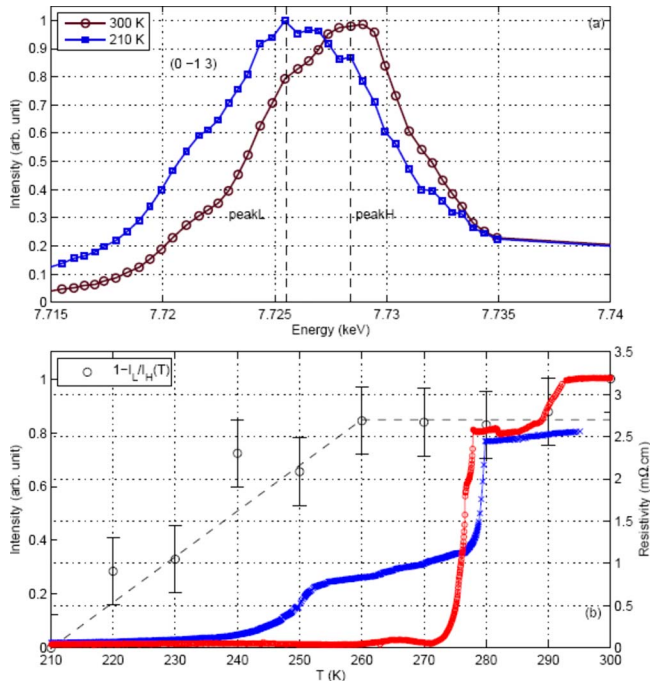


FIG. 6. (Color online) (a) Zoom of the energy spectrum of the $(0\ \bar{1}\ 3)$ superstructure reflection around the Co K edge. The two components of the double anomalous peak are labeled peak L and peak H. (b) Temperature dependence of the intensity ratio of the low energy peak (peak L defined on top) to the high energy peak (peak H defined on the top), $(1 - I_L/I_H)$ (left scale) obtained upon heating. The resistivity curve from Fig. 1 is also plotted for comparison (right scale). Note that the resistivity and the intensity measurements have been performed on different crystals from the same batch. Fine differences between the Na concentrations cannot be excluded. Dashed lines are guide to the eyes.

to 290 K, the contribution of these two components progressively changes. Figure 6(b) displays the relative intensity of the higher energy peak to the lower energy peak $(1 - I_L/I_H)$ as a function of temperature. It gradually increases upon heating, but with a marked change in slope around 260 ± 10 K. For comparison, the heating resistivity curve from Fig. 1 is reproduced in Fig. 6. Note that anomalies in the $\rho(T)$ curve upon heating are observed at similar temperatures. The correlation between the steep increases in the thermal dependence of the resistivity (at $T \approx 265 \pm 2$ K and 275 ± 2 K) upon cooling and the steplike behavior of the thermal variation of $(1 - I_L/I_H)$ is fair although the measurements have been performed on different crystals with possible slight differences of Na concentrations. Interestingly, an analogous effect, attributed to a Na rearrangement has also been observed recently by x-ray powder diffraction, NMR, heat capacity, and transport measurements in the three-Co layers ($x=0.62$) (Ref. 8) and in the double-Co layers cobaltates ($x \sim 0.75$).^{9,11,15,18} These similar results are clear indications that the charge degrees of freedom originating from the Co layer are strongly connected to the Na ordering.

In conclusion, our results provide clear indications of a Co charge order surprisingly strong for a transition-metal

compound. The energy splitting of the two components of the double peak observed in the energy spectrum of the satellite reflections is comparable to the edge shift observed for cobaltates of different Co valences.³²

IV. CONCLUSIONS

We have characterized the Na and Co ordering in Na_xCoO_2 ($x \sim \frac{5}{6}$) by a combination of powerful experimental techniques including diffuse scattering and resonant anomalous scattering. The Na ordering is found to be already present at 300 K. Surprisingly, the Na patterning observed in our three Co-layers system is similar to that previously detected in double Co layers^{11,21} in spite of the different Na environment. However, for highly doped double Co-layers compounds, the Na environment is close to that of three Co-layers systems, because the Na(2) sites are nearly unoccupied. The structural similarities underlying the two types of Na cobaltates could explain their close physical properties. From the experimental data, we have provided a superlattice model formed of Na vacancy stripes in the (a, c) planes. This model differs starkly from those previously published^{11,21} even though the experimental data are, in appearance, similar. We believe that this disparity comes from the twinning effects that were systematically neglected in the previous works.

In addition to the determination of the Na pattern, we have measured the Co charge by x-ray anomalous scattering at the Co K edge. The spectra show a strong anomalous effect, fingerprint of a Co charge order. The anomalous effect can be decomposed into two components related to the two Co charge states. The relative weight of these two components presents a thermal dependence indicating a variation in the two Co charge states. Interestingly, this thermal dependence is very close to the thermal dependence of the resistivity. Both curves show an anomaly at 265 K certainly related to the Na rearrangement. Thus our study provides evidence of the tight connection between Na orderings and Co charge orders. Finally, we have proposed a model for the Co charge order that is consistent with all the presented experimental facts. In order to validate this model and quantify the Co charge order, a simulation of the anomalous intensity based on an accurate superstructure is necessary. Further work is in progress to refine the structure and to carry out the simulations.

ACKNOWLEDGMENTS

We acknowledge H. Alloul, J. Bobroff, G. Collin, T. Emge, and V. Heresanu for their help concerning the characterization step and for stimulating discussions. We also acknowledge the European Synchrotron Radiation Facility for provision of beam line and the ID20 team for its technical support. This work was partially supported by the National Science Foundation, Solid State Chemistry Grant, No. NSF-DMR-0541911 (for V.P. and M.G.) and by NFS/CNRS grant (for P.F.-L.).

- ¹M. G. S. R. Thomas, P. G. Bruce, and J. B. Goodenough, *Solid State Ionics* **17**, 13 (1985).
- ²J. Molenda, C. Delmas, P. Dordor, and A. Stoklosa, *Solid State Ionics* **12**, 473 (1984).
- ³I. Terasaki, Y. Sasago, and K. Uchinokura, *Phys. Rev. B* **56**, R12685 (1997).
- ⁴K. Takada, H. Sakurai, E. Takayama-Muromachi, F. Izumi, R. A. Dilanian, and T. Sasaki, *Nature (London)* **422**, 53 (2003).
- ⁵D. J. Singh, *Phys. Rev. B* **61**, 13397 (2000).
- ⁶K. W. Lee, J. Kunes, and W. E. Pickett, *Phys. Rev. B* **70**, 045104 (2004).
- ⁷Y. Wang, N. Rogado, R. Cava, and N. Ong, *Nature (London)* **423**, 425 (2003).
- ⁸M. Blangero, D. Carlier, M. Pollet, J. Darriet, C. Delmas, and J.-P. Doumerc, *Phys. Rev. B* **77**, 184116 (2008).
- ⁹Q. Huang, B. Khaykovich, F. C. Chou, J. H. Cho, J. W. Lynn, and Y. S. Lee, *Phys. Rev. B* **70**, 134115 (2004).
- ¹⁰T. Zhou, A. J. Wright, D. Zhang, T. W. Button, and C. Greaves, *J. Mater. Chem.* **18**, 1342 (2008).
- ¹¹M. Roger, D. J. P. Morris, D. A. Tennant, M. J. Gutmann, J. P. Goff, J.-U. Hoffmann, R. Feyerherm, E. Dudzik, D. Prabhakaran, A. T. Boothroyd, N. Shannon, B. Lake, and P. P. Deen, *Nature (London)* **445**, 631 (2007).
- ¹²M. Blangero, R. Decourt, D. Carlier, G. Ceder, M. Pollet, J.-P. Doumerc, J. Darriet, and C. Delmas, *Inorg. Chem.* **44**, 9299 (2005).
- ¹³Y. S. Meng, A. Van der Ven, M. K. Y. Chan, and G. Ceder, *Phys. Rev. B* **72**, 172103 (2005).
- ¹⁴I. R. Mukhamedshin, H. Alloul, G. Collin, and N. Blanchard, *Phys. Rev. Lett.* **93**, 167601 (2004).
- ¹⁵J. L. Gavilano, D. Rau, B. Pedrini, J. Hinderer, H. R. Ott, S. M. Kazakov, J. Karpinski, *Phys. Rev. B* **69**, 100404(R) (2004).
- ¹⁶I. R. Mukhamedshin, H. Alloul, G. Collin, and N. Blanchard, *Phys. Rev. Lett.* **94**, 247602 (2005).
- ¹⁷M. H. Julien, C. de Vaulx, H. Mayaffre, C. Berthier, M. Horvatic, V. Simonet, J. Wooldridge, G. Balakrishnan, M. R. Lees, D. P. Chen, C. T. Lin, and P. Lejay, *Phys. Rev. Lett.* **100**, 096405 (2008).
- ¹⁸B. C. Sales, R. J. Jin, K. A. Affholter, P. Khalifah, G. M. Veith, and D. Mandrus, *Phys. Rev. B* **70**, 174419 (2004).
- ¹⁹H. W. Zandbergen, M. L. Foo, Q. Xu, V. Kumar, and R. J. Cava, *Phys. Rev. B* **70**, 024101 (2004).
- ²⁰G. Collin, N. Blanchard, and H. Alloul (unpublished).
- ²¹F. C. Chou, M. W. Chu, G. J. Shu, F. T. Huang, W. W. Pai, H. S. Sheu, and P. A. Lee, *Phys. Rev. Lett.* **101**, 127404 (2008).
- ²²J. Geck, M. v. Zimmermann, H. Berger, S. V. Borisenko, H. Eschrig, K. Koepf, M. Knupfer, and B. Büchner, *Phys. Rev. Lett.* **97**, 106403 (2006).
- ²³L. Viciu, J. W. G. Bos, H. W. Zandbergen, Q. Huang, M. L. Foo, S. Ishiwata, A. P. Ramirez, M. Lee, N. P. Ong, and R. J. Cava, *Phys. Rev. B* **73**, 174104 (2006).
- ²⁴D. P. Chen, X. Wang, C. T. Lin, and S. X. Dou, *Phys. Rev. B* **76**, 134511 (2007).
- ²⁵Y. Takahashi, Y. Gotoh, and J. Akimoto, *J. Solid State Chem.* **172**, 22 (2003).
- ²⁶F. C. Chou, G. J. Shu, F. -T. Huang, M. -W. Chu, J. -Y. Lin, and P. A. Lee, arXiv:0901.0622 (unpublished).
- ²⁷G. Lang, J. Bobroff, H. Alloul, P. Mendels, N. Blanchard, and G. Collin, *Phys. Rev. B* **72**, 094404 (2005).
- ²⁸Y. Joly, S. Grenier, and J. E. Lorenzo, *Phys. Rev. B* **68**, 104412 (2003).
- ²⁹S. Fagot, P. Foury-Leykian, S. Ravy, J. P. Pouget, E. Lorenzo, Y. Joly, M. Greenblatt, M. V. Lobanov, and G. Popov, *Phys. Rev. B* **73**, 033102 (2006).
- ³⁰L. Paolasini, C. Detlefs, C. Mazzoli, S. Wilkins, P. P. Deen, A. Bombardi, N. Kernavanois, F. de Bergevin, F. Yakhou, J. P. Valade, I. Breslavetz, A. Fondacaro, G. Pepellin, and P. Bernard, *J. Synchrotron Radiat.* **14**, 301 (2007).
- ³¹Ph. Leininger, J.-P. Rueff, J.-M. Mariot, A. Yaresko, O. Proux, J.-L. Hazemann, G. Vankó, T. Sasaki, and H. Ishii, *Phys. Rev. B* **74**, 075108 (2006).
- ³²V. V. Poltavets, M. Croft, and M. Greenblatt, *Phys. Rev. B* **74**, 125103 (2006).